Role of Magnesium in Nucleotide Exchange on the Small G Protein Rac Investigated Using Novel Fluorescent Guanine Nucleotide Analogues†

Adam Shutes, Robert A. Phillips, John E. T. Corrie, and Martin R. Webb*

National Institute for Medical Research, Mill Hill, London NW7 1AA, U.K.

Received October 18, 2001; Revised Manuscript Received January 17, 2002

ABSTRACT: Novel guanine nucleotide analogues have been used to investigate the role of Mg^{2+} in nucleotide release and binding with the small G protein rac. The fluorescent analogues have 7-(ethylamino)-8-bromocoumarin-3-carboxylic acid attached to the 3′-position of the ribose via an ethylenediamine linker. This modification has only small effects on the interaction with rac. There are large fluorescence changes on binding of the triphosphate to rac, on hydrolysis, and then on release of the diphosphate. Furthermore, the fluorescence is sensitive to the presence of Mg^{2+} in the active site. Using this signal, it was shown that, for a variety of conditions, the nucleotides dissociate by a two-step mechanism. Mg^{2+} is released first followed by the nucleotide. With the diphosphate, Mg^{2+} is fast and nucleotide release slow. For the fluorescent GMPPNP analogue, the rate of dissociation is limited by Mg^{2+} release. In the latter case, Mg^{2+} binds tightly with a K_d of 61 nM, whereas for the diphosphate the K_d is 11 μM (30 °C, pH 7.6).

The metal ion Mg^{2+} plays an essential role in a wide range of biological processes. The role of metal ions in the binding of purine nucleotide to proteins and in subsequent phosphotransfer reactions has been well characterized both by solution biochemistry and by a range of physical techniques, such as EPR, using Mn^{2+} as an analogue of magnesium (*1*−*3*), and crystal stucture determination (*4*). These studies have provided detailed information about the coordination of Mg^{2+}, for example, the identity of phosphate oxygens and amino acids coordinated to the metal. In general, enzymes in which the terminal phosphate of GTP or ATP is hydrolyzed or transferred have Mg^{2+} bound to both β- and γ-phosphates in the nucleoside triphosphate complex. In the product diphosphate complex, Mg^{2+} binds to the β-phosphate. Structural information has led to models of how the Mg^{2+} might be involved in enzymic catalysis. For example, coordination to the β-phosphate helps to neutralize charge on ADP, making it a better leaving group from the terminal phosphate. Despite this information, the details of the Mg^{2+} involvement in enzymic mechanisms are often elusive, in part because of the lack of suitable methods to probe this involvement. Thus the role of Mg^{2+} may be not included in a described mechanism, despite it being an essential cofactor. An exception to this is the description of Mg^{2+} involvement in the GTPase mechanism of the small G protein ras (*5*, *6*).

For many triphosphatases and phosphotransferases, binding of substrate and release of products are relatively rapid processes. However, small G proteins bind both GTP and GDP very tightly under physiological conditions, typically with dissociation constants that are nanomolar to picomolar (*6*−*8*). Release of nucleotide is very slow in the absence of added factors but is catalyzed by protein exchange factors (GEFs) in vivo (*9*). These GEFs play a role in controlling what nucleotide is bound to the small G protein. Other proteins involved in this control are the GTPase activating proteins (GAPs) that accelerate the GTPase rate by several orders of magnitude (*10*). The phosphorylation state of the nucleotide (GTP or GDP) determines the activity of the small G proteins with respect to effectors downstream on the signaling pathway with GTP-bound forms being active and GDP forms inactive.

In the case of the small G protein rac, Mg^{2+} is coordinated to GTP at the β- and γ-phosphate oxygens (*11*). In addition, it is bound to T17, T35, and two water oxygens. In the diphosphate complex, the coordination to the γ-oxygen is replaced by another water (M. Hirshberg and M. R. Webb, unpublished result). Free in solution, Mg^{2+} binds to the polyphosphate chains of nucleotides with an overall K_d of ∼0.1 mM (for ATP, pH 7.2) (*12*, *13*). Unlike the situation when the complex is protein-bound, several different coordination isomers are in equilibrium (e.g., $\alpha\beta\gamma$ tridentate and various bidentates).

In the presence of millimolar Mg^{2+}, nucleotide exchange on most small G proteins, including rac, is very slow. The exchange can be accelerated by the presence of ammonium sulfate and/or by reducing the concentration of free Mg^{2+}, for example, by the use of EDTA (*14*). Because nucleotides bind very tightly to small G proteins, net release of a particular nucleotide from its complex with the protein is achieved by exchanging with a large excess of another nucleotide that is initially free in solution.

Here we describe the use of GTP and GDP analogues labeled with a fluorescent coumarin via an ethylenediamine linker attached to the 3′-oxygen of ribose (*15*, *16*). Labeling in this position generally has little effect on the interaction of the nucleotide with ATPases or GTPases but can provide a reporter group for the interaction (*17*). In the case of rac, as with various other GTPases and ATPases, the crystal structure shows the 3′-hydroxyl of the nucleotide exposed

† This work was supported by the Medical Research Council, U.K.

* To whom correspondence should be addressed. Tel: (44) 20 8959 3666. Fax: (44) 20 8906 4477. E-mail: mwebb@nimr.mrc.ac.uk.

10.1021/bi0119464 CCC: $22.00
Published on Web 02/22/2002

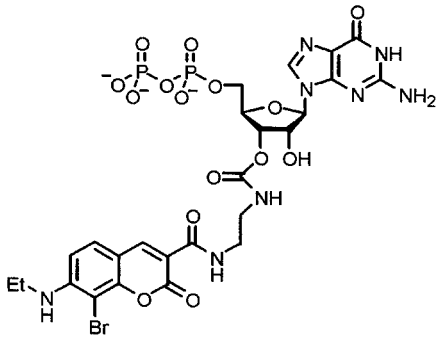

FIGURE 1: Structure of 3′-mbc-edaGDP.

on the surface (*11*). Conjugates were prepared with three different coumarins, 7-(diethylamino)coumarin-3-carboxylic acid, coumarin 343,[1] and 7-(ethylamino)-8-bromocoumarin-3-carboxylate (*18*). Only the last conjugate (mbc-edaGDP, Figure 1) gives a large fluorescence change on binding to rac or on dissociation of the rac−nucleotide complex. In addition, the fluorescence of mbc-edaGTP and the equivalent diphosphate responds to the presence of Mg^{2+} in the active site: there is a fluorescence change when Mg^{2+} binds to the rac−nucleotide complex. These fluorescence signals have enabled us to probe the role of this metal ion in the nucleotide release reaction. The other conjugates are not described in detail.

EXPERIMENTAL PROCEDURES

Materials. Rac1 was prepared using a GST-fusion expression system followed by cleavage from the GST (*19*) and is referred to as "rac" elsewhere in this work. The phosphate sensor MDCC-PBP was prepared and used as described (*20*).

Mbc-edaGTP and -edaGDP were synthesized and characterized as described for the ATP analogues (*16*). EdaGMPPNP was synthesized by a similar route but slightly different experimental protocol. The changes are described below. Following coupling of ethylenediamine to GMPPNP activated by carbonyldiimidazole, the unwanted modification to the terminal phosphate was removed by incubation for 16 h at pH 2.5 and room temperature, as opposed to a similar treatment at 4 °C, which is sufficient treatment for ATP or GTP. Coupling of the coumarincarboxylic acid was then as described (*16*). HPLC analysis of edaGMPPNP used a Partisil SAX column (Whatman, 0.4 cm × 25 cm) with mobile phase 0.4 M $(NH_4)_2HPO_4$, adjusted to pH 4.0 with concentrated HCl, running at 2 mL min^{-1}, monitored at 252 nm. Mbc-edaGMPPNP was analyzed by HPLC on a Partisphere SAX column (Whatman, 12.5 cm × 0.45 cm). The mobile phase at 1.5 mL min^{-1} was 0.35 M $(NH_4)_2HPO_4$, adjusted to pH 4.0 with concentrated HCl (75% v/v), with methanol (25%). Other coumarin conjugates were prepared by equivalent procedures.

[1] Abbreviations: edaGTP, 2′(3′)-*O*-[*N*-(2-aminoethyl)carbamoyl]-GTP; deac-edaGTP, 2′(3)-*O*-{*N*-[2-(7-(diethylamino)coumarin-3-carboxamido)ethyl]carbamoyl}GTP; but-edaGTP, coumarin 343-edaGTP; coumarin 343, 2,3,6,7-tetrahydro-11-oxo-1*H*,5*H*,11*H*-[1]benzopyrano-[6,7,8-*ij*]quinolizine-10-carboxylic acid; mbc-edaGTP, 2′(3′)-*O*-{*N*-[2-(7-(ethylamino)-8-bromocoumarin-3-carboxamido)ethyl]carbamoyl}-GTP; MDCC, *N*-[2-(1-maleimidyl)ethyl]-7-(diethylamino)coumarin-3-carboxamide; MDCC-PBP, A197C mutant of phosphate binding protein of *Escherichia coli* labeled with MDCC; mantGDP; 2′(3′)-*O*-(*N*-methylanthraniloyl)GDP.

Complexes of rac with specific nucleotides were prepared by exchange in the presence of EDTA and/or ammonium sulfate as described (*11*, *19*). The mbc-nucleotide bound to rac was analyzed by HPLC on a Partisphere SAX column (Whatman, 12.5 cm × 0.45 cm), following an acid quench in a large excess of the mobile phase buffer. The mobile phase at 1.5 mL min^{-1} was 0.5 M $(NH_4)_2HPO_4$, adjusted to pH 4.0 with concentrated HCl, (75% v/v) with methanol (25%).

Other Measurements. Absorbance spectra were obtained on a Beckman DU640 spectrophotometer. Fluorescence measurements were obtained on a Perkin-Elmer LS50B fluorometer with xenon lamp. Stopped-flow experiments were carried out in a HiTech SF61MX apparatus, with a mercury−xenon lamp and HiTech IS-2 software. For mbc fluorescence, there was a monochromator with 7 nm slits on the excitation light (406 nm) and a 435 nm cutoff filter on the emission. Fluorescence anisotropy was measured with this instrument in the "T" format, allowing simultaneous acquisition of horizontal ($I_{||}$) and perpendicular ($I_{\perp}$) components. Anisotropy is $(I_{||} - I_{\perp})/(I_{||} + 2I_{\perp})$. All measurements were at 30 °C in 20 mM Tris·HCl, 20 mM ammonium sulfate, and 1 mM $MgCl_2$ or 10 mM EDTA, with final pH 7.5, unless otherwise stated. Concentrations are those in the mixing chamber except where stated. Data were fitted to theoretical curves using the HiTech software or Grafit (*21*).

Conditions to obtain "Mg-free" rac complexes were determined by titrating the fluorescence of the complex with increasing amounts of EDTA. This gave a minimum concentration of EDTA necessary to give ∼75% Mg-free complex for a particular batch of complex. This procedure is empirical, because of a varying and unknown amount of remnant Mg^{2+} with the complex, even when it is purified by gel filtration in the absence of added Mg^{2+}. For rac·mbc-edaGDP 20 μM EDTA was sufficient, but for rac·mbc-edaGMPPNP 0.5 mM EDTA was required. In the latter case, there is considerable uncertainty in defining the free Mg^{2+} concentration at low added Mg^{2+} because of competition between EDTA and rac for Mg^{2+} binding.

RESULTS

Synthesis and Fluorescence of the Nucleotide Analogues. Mbc-edaGTP, -edaGDP, and -edaGMPPNP have been synthesized via the eda-nucleotides using the method described for the coumarin-labeled ATP analogues but with minor modifications as described here in the Experimental Procedures (*16*). The equivalent nucleotide analogues containing two other coumarins were also prepared, namely, deac-edaGTP and but-edaGTP. The synthesis produces a mixture of isomers that have the linker attached to either the 2′- or 3′-position of the ribose but interconvert only very slowly (*16*). So the nucleotides could be isolated as the separate isomers by ion-exchange chromatography. To determine the relative affinity for rac of the isomers of these analogues, GDP bound to rac was exchanged using a mixture of isomers. HPLC analysis showed that rac binds the 3′-isomer preferentially (>90%) so in this work only the 3′-isomer is used.

For deac-edaGDP and but-edaGDP, the fluorescence quantum yields and spectra are the same as those for the equivalent adenine nucleotides (*16*). That is not the case for

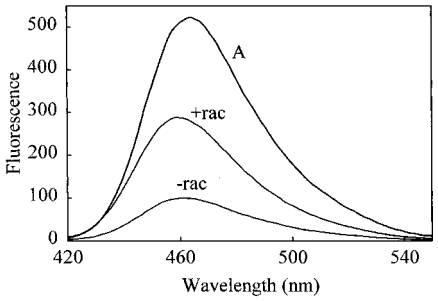

FIGURE 2: Fluorescence emission spectra. Data are for mbc-edaGDP free in solution and complexed with rac. The emission spectrum of mbc-edaATP (A) is shown for comparison. All nucleotide concentrations were 0.5 μM, and the spectra were measured in 20 mM Tris·HCl, pH 7.6, and 0.5 mM $MgCl_2$.

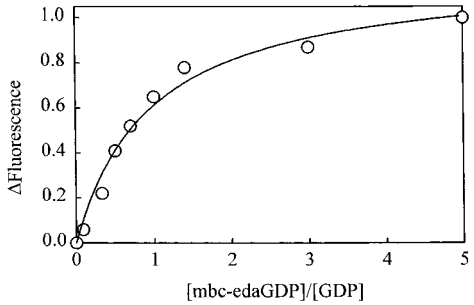

FIGURE 3: Relative affinity of mbc-edaGDP and GDP for rac. The size of the fluorescence change was measured on binding mbc-edaGDP to rac in the presence of different amounts of GDP. rac·GDP (0.1 μM) was incubated with 0.5 μM free nucleotide consisting of different proportions of GDP and mbc-edaGDP, so the total nucleotide is 0.6 μM. The solution was in 20 mM Tris·HCl, pH 7.5, 20 mM ammonium sulfate, and 5 mM EDTA. The fluorescence change was normalized to the value at 0.5 μM mbc-edaGDP. The data were fit to the equation for the proportion of rac bound with mbc-edaGDP = $ND/(K' + D)$, where N is the normalization factor, D is the ratio of nucleotides and K' is the ratio of dissociation constants (mbc-edaGDP/GDP). The best fit curve gives a value of 0.96 for K'.

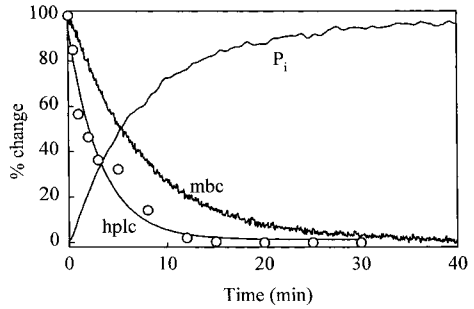

FIGURE 4: Hydrolysis of rac·Mg·mbc-edaGTP. Mbc fluorescence was followed at 30 °C for a solution of 0.5 μM rac·mbc-edaGTP in 20 mM Tris·HCl, pH 7.5, 20 mM ammonium sulfate, and 0.5 mM $MgCl_2$. An approximately equal amount of rac·mbc-edaGDP was also present at zero time. Excitation was at 406 nm and emission at 460 nm. In a separate measurement, P_i release was followed in the presence of 15 μM MDCC-PBP (*20*). In this case, excitation was at 450 nm, away from the MDCC maximum (420−430 nm) in order to minimize excitation of the mbc (excitation maximum 405 nm). Emission was measured at 470 nm. A control experiment showed that, with these wavelengths, the fluorescence change due to mbc excitation was <10% of that due to MDCC excitation. The progress of hydrolysis was also measured by HPLC to determine the ratio of mbc-edaGTP to mbc-edaGDP. All data are plotted as percentage of the total change to allow direct comparison. The best fit exponentials gave 0.31 min^{-1} for the HPLC data, 0.139 min^{-1} for the P_i assay, and 0.136 min^{-1} for mbc fluorescence.

mbc-edaGDP: the quantum yield of mbc-edaADP is 0.6, whereas for the guanosine analogue it is 5-fold less, and this is reflected in the fluorescence spectra (Figure 2). The fluorescence spectra and quantum yields of mbc-edaGTP, -edaGDP, and -edaGMPPNP free in solution are identical to each other, are unaffected by the presence of EDTA or Mg^{2+}, and are not sensitive to buffer conditions at a fixed pH. In addition, the presence of 0.5 mM GDP has no affect on the emission spectrum of mbc-edaGDP, suggesting that the reduction in fluorescence relative to the adenine analogues may not be due to intermolecular interaction between guanine base and coumarin.

Mbc-edaGTP and -edaGDP with Rac. When bound to rac, the fluorescence intensities of deac-edaGDP and but-edaGDP increase only slightly (~20%; data not shown), but that of mbc-edaGDP increases 3-fold (Figure 2). We show below that the fluorescence of the bound mbc-nucleotide depends on the presence of Mg^{2+} and on whether the nucleotide is a diphosphate or triphosphate.

It is important to know how well these analogues mimic natural nucleotides in their interaction with rac. To assess the validity of our measurements with the mbc-nucleotides, the relative affinities of mbc-edaGDP and GDP for rac in the presence of EDTA were determined by the measurement of the fluorescence increase due to mbc-edaGDP binding in competition with different amounts of GDP (Figure 3). This shows that the dissociation constant of the analogue is 0.96 that of GDP. In the presence of Mg^{2+}, mbc-edaGDP, mbc-edaGMPPNP, GDP, and GMPPNP all have similar affinity for rac as shown by a similar competition binding assay (data not shown). The hydrolysis rate of rac·mbc-edaGTP is similar to that of GTP as described below. The release of mbc-edaGDP is ~4-fold slower than that of GDP (see below).

Mbc-edaGTP Hydrolysis. The rac·mbc-edaGTP complex was prepared by nucleotide exchange. In practice, only ~50% of the rac has mbc-edaGTP bound after this procedure, the remainder being diphosphate because of hydrolysis during exchange and purification. The hydrolysis of rac·mbc-edaGTP in buffer containing Mg^{2+} was then followed as a function of time by two methods (Figure 4). First, P_i release kinetics were measured using the fluorescent P_i sensor MDCC-PBP (*20*). The time course of hydrolysis was also followed by HPLC analysis of nucleotide to measure the ratio of mbc-edaGDP/mbc-edaGTP at particular times. These two methods gave different rates at 30 °C: 0.136 min^{-1} from P_i measurement and 0.31 min^{-1} from HPLC, indicative that the cleavage step is 2-fold faster than the subsequent step in which P_i is released. This will be discussed later. In comparison, HPLC data with rac·GTP (not shown) gave a rate of 0.42 min^{-1}. During the hydrolysis of mbc-edaGTP, the mbc fluorescence changed with a rate of 0.139 min^{-1}, almost identical to that of P_i release, suggesting that the mbc fluorescence reports P_i release from the catalytic site. After correction for the initial proportion of triphosphate in the rac complex, the fluorescence of rac·mbc-edaGTP is 2.6-fold greater than for rac·mbc-edaGDP.

Mbc-edaGDP Dissociation from Rac. Dissociation of the labeled nucleotide was achieved by rapidly mixing a solution of rac·mbc-edaGDP containing Mg^{2+} (i.e., the rac·Mg·mbc-edaGDP complex) with one containing excess GDP and EDTA. The reaction was performed in a stopped-flow

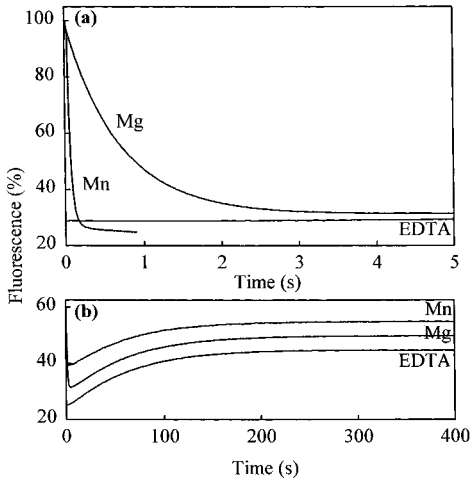

FIGURE 5: Fluorescence changes during nucleotide release from rac·mbc-edaGDP complexes. Rac·mbc-edaGDP (2 μM) was rapidly mixed with 200 μM GDP and 10 mM EDTA (syringe concentrations; mixing chamber concentrations are half these values). When the complex was in the Mg form, 0.5 mM $MgCl_2$ was present. For the Mg-free form, 10 mM EDTA was present with the protein complex. The Mn form was with 0.5 mM $MnCl_2$. The data are shown over short (a) and long (b) time scales but at the same ordinate expansion. In (b) the other data are offset by 5% from the Mg trace, which was normalized to 100% at zero time. The curves were fit to single exponentials; see text for details.

apparatus, and the fluorescence change with time was biphasic (Figure 5). The fast phase (Figure 5a) was a large fluorescence decrease that fitted well to a single exponential. This was followed by a much smaller and slower fluorescence rise (Figure 5b), also well fitted by a single exponential.

To relate the fluorescence changes to biochemical processes, several measurements were performed. The dissociation protocol was repeated but using rac·mbc-edaGDP initially in the presence of excess EDTA instead of Mg^{2+}. With these conditions, the first phase was abolished, but the fluorescence rise was very similar to the second phase with Mg^{2+} (Figure 5). These data are interpreted as being due to a mechanism of nucleotide release in which Mg^{2+} is released prior to the nucleotide:

$$\text{rac·Mg·mbc-edaGDP} \underset{1}{\overset{-Mg^{2+}}{\rightleftharpoons}} \text{rac·mbc-edaGDP} \underset{2}{\rightleftharpoons} \text{rac} + \text{mbc-edaGDP} \quad (1)$$

In this equation, the forward and reverse rate constants and the equilibrium constant for any step i are given by k_{+i}, k_{-i}, and K_i, respectively. The large fluorescence decrease is on step 1, which has a rate constant of 1.45 s^{-1} (k_{+1}). The subsequent smaller fluorescence rise is on step 2, which has a rate constant of 0.016 s^{-1} (k_{+2}). Rate constants are summarized in Table 1.

When the exchange was done with rac initially in the presence of EDTA, a single slow process was observed with a rate constant of 0.016 s^{-1}, interpreted as being due to step 2. When rac·Mg·mbc-edaGDP was mixed with EDTA but free GDP was absent, the slow second phase was not observed. The single fast phase had a rate constant of 1.60 s^{-1} (data not shown), consistent with observing Mg^{2+} release from rac but not release of the mbc-edaGDP. Nucleotide release would only occur to very limited extent, in the absence of excess, free GDP to replace it in the catalytic

Table 1: Summary of Rate Constants for the Two Steps in Eq 1[a]

nucleotide	salt[b]	metal ion	k_{+1} (s^{-1})	k_{+2} (s^{-1})
Mbc-edaGDP	$(NH_4)_2SO_4$	Mg^{2+}	1.45	0.016
Mbc-edaGDP	$(NH_4)_2SO_4$	Mn^{2+}	25.0	0.016
Mbc-edaGDP	KCl	Mg^{2+}	1.51	0.033
Mbc-edaGDP	KCl	Mn^{2+}	15.2	0.032
Mbc-edaGMPPNP	$(NH_4)_2SO_4$	Mg^{2+}	0.0096	3.5/0.26[c]
Mbc-edaGMPPNP	$(NH_4)_2SO_4$	Mn^{2+}	0.091	3.8/0.35[c]
Mbc-edaGMPPNP	KCl	Mg^{2+}	0.0037	8.5
Mbc-edaGMPPNP	KCl	Mn^{2+}	0.014	12.4

[a] Rate constants are reported for fluorescence intensity changes as described in the text. [b] 20 mM ammonium sulfate or 50 mM KCl was used. [c] These traces were biphasic with the faster phase having much larger amplitude.

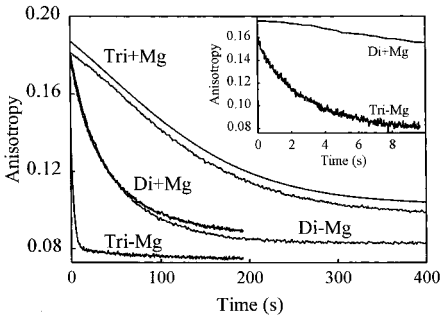

FIGURE 6: Anisotropy changes during mbc-nucleotide release from rac. Solution conditions were as in Figure 5. Rac·mbc-edaGDP was preincubated with Mg^{2+} (Di + Mg) or EDTA (Di − Mg) prior to mixing with excess GDP and EDTA. Tri + Mg and Tri − Mg similarly refer to rac·mbc-edaGMPPNP. The inset shows two traces on a faster time scale. The anisotropy observed at a particular time point is the average for the starting and finishing species, weighted by the relative fluorescence intensity of the two species as well as their relative concentrations. In most cases here, the anisotropy change is being measured for a process where there is only a small fluorescence intensity change, and so the data were fit to exponentials, ignoring the small effect due to the fluorescence weighting. These gave 0.024 s^{-1} (Di + Mg), 0.021 s^{-1} (Di − Mg), and 0.37 s^{-1} (Tri − Mg). For rac·Mg^{2+}·mbc-edaGMPPNP (Tri + Mg) there is a large fluorescence change (~3-fold decrease, as shown in Figure 8). In this case the data were fit to the equation described by Eccleston et al. (*31*), which includes the weighting for relative fluorescence. The best fit curve is shown offset by 0.005 for clarity. This gave a rate constant of 0.012 s^{-1}.

site of rac. To test this interpretation of eq 1, the exchange was repeated using Mn^{2+}, which is a reasonably good analogue of Mg^{2+} (*1*, *8*, *22*). In this case, the first phase was faster (25 s^{-1}) than with Mg^{2+} but had a similar amplitude (Figure 5). The second phase was very similar to that observed with Mg^{2+}. This suggests that the first phase corresponds to the release of metal ion and that this rate depends on the identity of that ion.

Finally, the reactions in the presence of Mg^{2+} or EDTA were repeated but following fluorescence anisotropy with time (Figure 6). Similar, single exponential changes were seen whether or not the rac·mbc-edaGDP complex has Mg^{2+} bound initially. The rate constants were similar to those obtained for the slow phase when measuring fluorescence intensity. When Mn^{2+} was the divalent cation, a similar trace was also observed (data not shown). In none of these anisotropy traces was a fast phase observed. The anisotropy measurements support the mechanism of eq 1 because rotational correlation time is a major determinant of anisotropy. Therefore, assuming that global motion of the complex containing the fluorophore dominates total motion of the

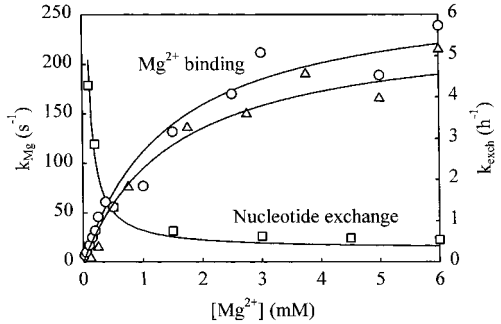

FIGURE 7: Rates of Mg^{2+} binding and nucleotide exchange as a function of Mg^{2+} concentration. The rate of Mg^{2+} binding was measured by mixing 0.5 μM rac·mbc-edaGDP (circles) or rac·mbc-edaGMPPNP (triangles) in the presence of minimum EDTA with different concentrations of $MgCl_2$ (no EDTA) at the concentrations shown. The fluorescence changes were fit to single (GDP) or double (GMPPNP) exponentials to obtain the values of k_{Mg} shown. These values were then fit to hyperbolas to give values for the equivalent of eq 2 of $1/K_{1a}$ of 2.2 mM (GDP analogue) and 1.5 mM (GMPPNP). $k_{+1b} + k_{-1b}$ is 304 s^{-1} for GDP and 237 s^{-1} for GMPPNP. Nucleotide exchange was measured using 0.1 μM rac·mbc-edaGDP and 100 μM GDP at different Mg^{2+} concentrations. The fluorescence changes were fit to single exponentials to obtain values for k_{exch}. The theoretical curve is calculated from the values of rate constants obtained for eqs 1 and 2. See text for details.

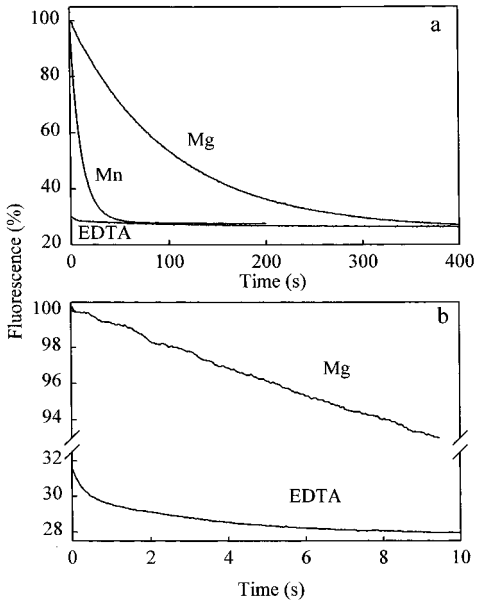

FIGURE 8: Fluorescence changes during nucleotide release from rac·mbc-edaGMPPNP complexes. Data were obtained as in Figure 5, and the same measurements are shown in panels a and b but on different time scales. The trace for nucleotide displacement from rac·mbc-edaGMPPNP in the presence of EDTA was biphasic, with rate constants of 0.27 and 3.6 s^{-1}. The rate constants were 0.0096 s^{-1} when the process was measured in the presence of Mg^{2+} and 0.091 s^{-1} in the presence of Mn^{2+}.

fluorophore, the measured values of anisotropy will be determined largely by the size of the complex. In such a case, the main change in anisotropy would be on step 2 of eq 1. The rate constants observed using anisotropy are in agreement with this, being close to those ascribed to step 2 from intensity measurements.

All of the above measurements were performed in the presence of 20 mM ammonium sulfate, which generally accelerates the exchange, so that it occurs over a time period relatively amenable for study. Key measurements were repeated in the absence of ammonium sulfate but with KCl in the reaction medium. Qualitatively, the same observations were made, but the relative amplitudes of the two phases of fluorescence changes were altered. In the case of mbc-edaGDP release (step 2, eq 1), there was a small fluorescence increase with ammonium sulfate present but a decrease with KCl present. The rate constants at 50 mM KCl are shown in Table 1. The hydrolysis was also followed by mbc fluorescence with KCl as the salt. Between 50 and 200 mM KCl, the rates were very similar to those in the presence of ammonium sulfate, but the amplitude decreased with increasing KCl concentration.

Finally, the measurements in Figure 5, with or without Mg^{2+}, were repeated using the T35A mutant of rac. In this case, the results (not shown) were similar whether or not Mg^{2+} was initially present with the complex. One slow phase was observed, suggesting either that Mg^{2+} was not bound initially or that the fluorescence was no longer sensitive to bound Mg^{2+}.

Mg^{2+} Binding to Rac·mbc-edaGDP. The kinetics of Mg^{2+} binding were measured over a range of Mg^{2+} concentrations by mixing Mg^{2+} with rac·mbc-edaGDP and following fluorescence with time (Figure 7). The complex was prepared in the presence of a concentration of EDTA as low as possible, while obtaining most of the complex Mg^{2+}-free. This EDTA concentration was determined by titrating EDTA into rac·mbc-edaGDP and following fluorescence as the EDTA removes the Mg^{2+} from the complex (see Experimental Procedures).

The traces of fluorescence increase with time for Mg^{2+} binding were fitted to single exponentials. The rate increased hyperbolically with Mg^{2+} concentration, and so the data were fitted to a two-step binding model:

$$Mg^{2+} + \text{rac·mbc-edaGDP} \underset{1a}{\rightleftharpoons} \text{rac·Mg·mbc-edaGDP} \underset{1b}{\rightleftharpoons} \text{rac·Mg·mbc-edaGDP*} \quad (2)$$

The fluorescence increase occurs on the second step, the asterisk designating a high fluorescence state. These two steps together are equivalent to the reverse of step 1 of eq 1.

Rate of Nucleotide Exchange as a Function of Mg^{2+} Concentration. The rate of nucleotide exchange was determined by following the fluorescence change with time over a range of Mg^{2+} concentrations while incubating rac·mbc-edaGDP with excess GDP (Figure 7). The rate decreased hyperbolically with concentration, as predicted from the mechanism described in eqs 1 and 2. This will be considered in detail in the Discusssion.

Rac·mbc-edaGMPPNP. The measurements described above were repeated with the nonhydrolyzable analogue of GTP, mbc-edaGMPPNP. Nucleotide release kinetics and the effect of divalent metals were very different from those seen with mbc-edaGDP (Figure 4) but were still consistent with the mechanism equivalent to eq 1.

When rac·Mg·mbc-edaGMPPNP was mixed with excess GDP and EDTA, a slow single phase decrease in fluorescence was observed (Figure 8). A single phase change with accelerated rate but the same amplitude was seen if the metal was Mn^{2+}. A fluorescence change with a similar rate and amplitude was observed when rac·Mg·mbc-edaGMPPNP was mixed with excess EDTA in the absence of GDP. The

slow single phase fluorescence change at 0.0096 s^{-1} presumably represents the slow dissociation of Mg^{2+} from the complex (step 1 of eq 1). This process is accelerated to 0.091 s^{-1} with Mn^{2+}. If no Mg^{2+} was present initially, when rac·mbc-edaGMPPNP was mixed with GDP, a much smaller, rapid and biphasic fluorescence decrease was observed (Figure 8b). The mbc-edaGMPPNP release (equivalent to step 2 of eq 1) is therefore accompanied by only a small fluorescence decrease,and the time course is relatively rapid. We will discuss later possible reasons why this is biphasic, unlike with the diphosphate.

Dissociation of nucleotide from rac·Mg·mbc-edaGMPPNP is limited by the slow rate of Mg^{2+} release, which is the step with the much larger fluorescence decrease. Anisotropy measurements are consistent with this (Figure 6). With Mg^{2+} present initially, a slow anisotropy decrease is observed, as nucleotide dissociation is the step likely to be responsible for the main change in anisotropy. With no Mg^{2+} present initially, the anisotropy change is fast, with a similar rate constant to the slower phase in the intensity trace.

The kinetics of Mg^{2+} binding to rac·mbc-edaGMPPNP were also measured in the same way as for the diphosphate (Figure 7). In this case, the preliminary titration required much more EDTA to strip Mg^{2+} from the complex initially than was the case with the diphosphate complex; see Experimental Procedures for details. The fluorescence rise on mixing Mg^{2+} with the Mg^{2+}-free complex was biphasic. There was a rapid phase with rates that were similar to those observed with mbc-edaGDP and varied with Mg^{2+} concentration. This was followed by a smaller, very slow phase with a rate (0.08 s^{-1}) independent of Mg^{2+} concentration. Figure 7 shows the dependence on Mg^{2+} concentration of the rate constant for the fast phase.

The rate of exchange was measured for rac·mbc-edaGMPPNP as a function of Mg^{2+} concentration. This also showed a hyperbolic dependence on concentration, but there are uncertainties about the exact free Mg concentrations at low values, as described above. In this case the observed rate was 2.7 h^{-1} at nominally 50 μM Mg^{2+}, and the rate was constant at 1.1 h^{-1} above 1 mM. It was not possible to model this exchange profile successfully at low Mg^{2+} concentrations, in part because of problems defining free Mg^{2+} concentrations and in part because of the biphasic traces on some measurements with the GMPPNP, as described above. However, at high concentration, the rate of exchange is consistent with the stepwise mechanism for dissociation of metal ion followed by nucleotide, as discussed later.

DISCUSSION

The measurement of fluorescence of mbc-labeled nucleotides during release from their complexes with rac suggests that stepwise dissociation of Mg^{2+} and then nucleotide occurs, as in eq 1. While this applies to both mbc-edaGDP and mbc-edaGMPPNP, these two nucleotides give very different fluorescence traces with different kinetics. First we discuss the evidence for this stepwise dissociation, then the implications for the factors determining the fluorescence of mbc-nucleotides when bound to rac, and finally the mechanism of nucleotide exchange.

Stepwise Dissociation of Mg^{2+} and Nucleotide. When mbc-labeled guanine nucleotides bind to rac, there is a fluorescence increase, the size of which depends both on the nucleotide state (di- or triphosphate) and on the presence of Mg^{2+}. Following the time course of mbc-edaGDP release from rac by fluorescence reveals two phases. The first phase is a large and relatively rapid decrease in fluorescence that depends both on the initial presence of divalent metal and on whether that metal is Mg^{2+} or Mn^{2+}. There is no change in anisotropy associated with this phase, suggesting that the nucleotide itself does not dissociate from the protein. Indeed, a similar fluorescence change is observed if the metal is complexed rapidly by EDTA without nucleotide exchange. This phase is therefore probably associated with Mg^{2+} release. The second phase is on a similar time scale to other measurements for nucleotide dissociation. This phase is independent of the divalent metal, has a large change in anisotropy associated with it, and is therefore probably associated with nucleotide dissociation. Thus for the diphosphate, rapid Mg^{2+} release is followed by slow nucleotide release as in eq 1.

When rac·mbc-edaGMPPNP dissociates, the fluorescence changes are consistent with slow Mg^{2+} release being followed by rapid nucleotide release. So when metal is present initially, nucleotide release is controlled by the slow rate of metal release: only one phase is seen in the fluorescence, a large decrease whose rate depends on whether the metal is Mg^{2+} or Mn^{2+}. If there is no metal present initially, only a small biphasic decrease in fluorescence is observed, which is likely to be associated with nucleotide dissociation. The amplitude of anisotropy change with the GMPPNP analogue is similar to that with the GDP analogue, but its rate depends on the presence of divalent metal ions, as expected. Nucleotide release (and so anisotropy change) is limited by the slow dissociation of the metal ion initially in the complex. When no metal is present, the anisotropy change presumably corresponds directly with the rate of nucleotide release. The biphasic nature of this process is discussed later.

In the presence of Mg^{2+}, mbc-edaGDP, mbc-edaGMPPNP, GDP, and GMPPNP all have similar affinity for rac. The similarity of the two mbc analogues is consistent with the overall rate of exchange in the presence of Mg^{2+} being similar, as seen in Figures 5 and 8. However, the GMPPNP binding affinity may not reflect that of GTP itself, as the differences in structure from the natural substrate on the phosphate chain may cause weaker binding of the analogue. This in turn may be reflected in differences in dissociation kinetics of GTP and GMPPNP from the protein. In the presence of EDTA, the relative affinity of the mbc-edaGMPPNP was difficult to determine because of the small signal change due to mbc-nucleotide binding in the absence of Mg^{2+}. In addition, the very tight binding of any residual Mg^{2+} to rac·mbc-edaGMPPNP causes a much larger signal that may mask that due to mbc-edaGMPPNP binding. However, a competition binding assay in the presence of EDTA is possible with mant-nucleotides. MantGDP binds approximately 2 orders of magnitude tighter than mant-GMPPNP (data not shown). The rapid release from rac of mbc-edaGMPPNP itself (step 2) relative to mbc-edaGDP is qualitatively consistent with this difference in affinities when no Mg^{2+} is bound.

The affinity of Mg^{2+} is likely to be less affected by the fact that GMPPNP is an analogue, as it is coordinated to oxygens of both protein and phosphate. With the extra O^-

coordinated to the metal, Mg^{2+} binds much tighter in the presence of GMPPNP than of GDP. On the basis of the rate and equilibrium constants obtained, the K_d for the mbc-edaGDP complex is 11 μM, and for the mbc-edaGMPPNP it is 0.061 μM. The difference is almost entirely due to the slower dissociation kinetics of the triphosphate and explains the difficulty of removing Mg^{2+} fully from the triphosphate complex.

Differences between Mg^{2+} and Mn^{2+}. There is a 10-fold increase in the rate of Mn^{2+} release from rac over that for Mg^{2+}. Such a change in rate might be expected because Mn^{2+} has a different ionic radius and therefore is presumably nonoptimal for the metal binding site. However, this change is a relatively small, consistent with Mn^{2+} being a good analogue of Mg^{2+} in nucleotide binding sites. The weaker binding suggests that the Mn^{2+} complex would be a useful intermediate to obtaining the metal-free triphosphate complex. The size of the fluorescence changes on removing Mn^{2+} is almost identical to that for Mg^{2+}, consistent with the structures of the complexes being very similar for the two metals and the mbc not reporting any difference.

Hydrolysis of Rac·mbc-edaGTP. There is an ~2-fold fluorescence decrease associated with hydrolysis or, more strictly, with the conversion from rac·Mg·mbc-edaGTP to rac·Mg·mbc-edaGDP. The time course of mbc fluorescence change follows closely that of P_i release rather than cleavage. Assuming that the hydrolysis follows the minimal mechanism of eq 3 and these two steps have equilibria well toward products, P_i release (step 4) is approximately 2-fold slower than the hydrolysis step per se (step 3).

$$R{\cdot}GTP \underset{3}{\rightleftharpoons} R{\cdot}GDP{\cdot}P_i \underset{4}{\rightleftharpoons} R{\cdot}GDP + P_i \qquad (3)$$

Mbc Fluorescence Depends on Mg^{2+} Coordination. The results presented here indicate that there is a relatively small change in fluorescence of mbc-nucleotides when they bind to rac. Such a change is observed with a variety of fluorescent nucleotides on binding to proteins (*17*), including the other coumarin analogues binding to rac, as mentioned above. Such changes may be ascribed to a gross change in environment on binding of the nucleotide to the protein. However, the fluorescence of rac·mbc-nucleotides depends largely on the presence of bound Mg^{2+} and the way it is coordinated to the phosphates. This coordination differs for the GDP and GTP states: the fluorescence of the triphosphate is 2.6-fold higher than the diphosphate when bound with Mg^{2+} to rac. Free in solution there is no difference in fluorescence of the di- and triphosphates. The relative fluorescence change on Mg^{2+} and nucleotide dissociation from rac depends on the salt conditions, although the kinetics themselves are not greatly affected above ~50 mM ionic strength.

The dependence of fluorescence on Mg^{2+} coordination may arise because the fluorophore interacts directly with an amino acid that is directly affected both by Mg^{2+} binding and by the change in coordination between GDP and GTP forms. Modeling the fluorophore onto the rac crystal structure does not reveal any probable site of interaction. The flexible diaminoethane linker means that the fluorophore could interact in many places on the surface. One possibility for interaction is T35, which is within the reach of the fluorophore when the nucleotide is bound. It is notably that, for rac·mbc-edaGDP, the rapid phase of fluorescence change during exchange (Figure 5) is lost for the T35A mutant, whereas the slow phase is little changed (data not shown). At this stage it is not known whether the first phase is lost because Mg^{2+} is only weakly bound or whether the fluorescence is no longer sensitive to Mg^{2+}, possibly because the coumarin no longer interacts with the amino acid at position 35. However, the whole of the effector loop (amino acids ~30−40) moves between the diphosphate and triphosphate structures (M. Hirshberg and M. R. Webb, unpublished result), so that any interaction of the fluorophore in this region would also change. Although the coordination between phosphate and metal is known for the GDP and GTP states, it is not so for the intermediate rac·GDP·P_i state. It seems likely, based on work with P_i analogues and on studies with other systems, that Mg^{2+} remains bound to P_i in this intermediate (*2*, *23*), and so the coordination would change only on P_i release. An alternative possible explanation for the dependence of fluorescence on Mg^{2+} coordination and nucleotide phosphorylation state is more indirect coupling of fluorophore and Mg^{2+}·nucleotide sites. The mbc could respond indirectly to the changes in conformation between the GDP-bound state, the GTP state, and the intermediates with no Mg^{2+} bound. In the case of the related rhoA, a structure has been determined for the GDP state with no Mg^{2+} bound (*24*), and this structure has large conformation differences from that with Mg^{2+} bound.

Another aspect of the fluorescence properties of the rac complex is why the mbc analogue gives rise to fluorescence changes not observed with the other coumarins. First, the mbc-labeled guanine nucleotides have much lower fluorescence than mbc itself or attached to other small molecules free in solution. Although the reason for this is not known, it means that the mbc can have a wide range of fluorescence values depending on its environment by a mechanism not shared by the other coumarins. This potentially gives mbc a greater sensitivity to environment than the others. Second, it is known that the conformation around the exocyclic amine plays a large role in the fluorescence intensity of coumarins (*25*−*27*). The presence of the bulky bromine atom next to this amine is presumably linked to the unusual properties of mbc. This bromine also provides a mode of interaction with specific amino acids, unavailable to the other coumarins. Such interactions could be readily transmitted to restrict or change the conformation of the coumarin amine. These questions on the detailed interaction of the coumarin with rac may potentially be answered by crystal structure data.

Mechanism of Nucleotide Exchange. A key question is whether the stepwise mechanism of nucleotide release, observed when Mg^{2+} is sequestered by EDTA, also holds under "normal" conditions of nucleotide exchange. This has been addressed, in particular for the diphosphate where a relatively complete set of rate constants has been determined for the kinetic mechanism of eq 1. The data in Figure 7 show that the rates of nucleotide exchange measured experimentally are consistent with those calculated for the stepwise mechanism over a wide range of Mg^{2+} concentrations.

For the GMPPNP analogue, some traces are biphasic, such as for Mg^{2+} binding and nucleotide release. This suggests that extra steps, such as conformational changes, may occur and so makes this analysis difficult. Further difficulties arise in assessing the free Mg^{2+} concentration at low values, because Mg^{2+} binds much tighter to rac·GMPPNP than to

rac·GDP. Assuming that the mechanism in eq 1 holds, nucleotide release at high Mg^{2+} concentration is given by $k_{+1}k_{+2}/k_{-1b}$. However, with mbc-GMPPNP, the fluorescence change occurs almost entirely on *net* Mg^{2+} release, and this may be controlled by the fast process of step 2 (3.6 s^{-1}, Figure 7), depending on the size of reverse rate constants. So the predicted rate of fluorescence change at 5 mM Mg^{2+} is (0.0096 × 3.6/160) s^{-1} = 0.78 h^{-1}. The measured rate is 1.1 h^{-1}, in reasonably good agreement.

In conclusion, the kinetic analysis using the mbc-labeled nucleotides has provided a detailed kinetic mechanism for nucleotide exchange for the basal reactions of rac. Nucleotide release can occur in two steps, with initial dissociation of Mg^{2+}. A similar situation occurs with ras (R. A. Phillips and M. R. Webb, unpublished data), suggesting that the mechanism might apply to a range of small G proteins. The results presented here provide a potential development of the mechanism of catalysis by exchange factors. There are a wide variety of such factors, and it has not been determined whether they share a common mechanism, as described for one (*28*). As the slow process in the exchange is loss of GDP, then this nucleotide release is accelerated by the exchange factors. The acceleration of nucleotide dissociation could be achieved in terms of eq 1 in two ways. The exchange factor could stabilize rac·GDP and so limiting rebinding of Mg^{2+} or it could accelerate the slow step 2. For at least two crystal structures of complexes of small G proteins with exchange factors, the exchange factor can be seen to disrupt the Mg^{2+} binding (*29*, *30*). Use of mbc-nucleotides presents a potential way to determine if the sequential dissociation of Mg^{2+} and nucleotide plays a role in the action of exchange factors.

ACKNOWLEDGMENT

We thank Dr. V. R. N. Munasinghe (NIMR, London) for supplies of 7-(ethylamino)-8-bromocoumarin-3-carboxylic acid.

REFERENCES

1. Reed, G. H., and Leyh, T. S. (1980) *Biochemistry 19*, 5472−5480.
2. Webb, M. R., Ash, D. E., Leyh, T. S., Trentham, D. R., and Reed, G. H. (1982) *J. Biol. Chem. 257*, 3068−3072.
3. Feuerstein, J., Kalbitzer, H. R., John, J., Goody, R. S., and Wittinghofer, A. (1987) *Eur. J. Biochem. 162*, 49−55.
4. Strang, S. R. (1997) *Annu. Rev. Biochem. 66*, 639−678.
5. John, J., Rensland, H., Schlichting, I., Vetter, I., Borasio, G. D., Goody, R. S., and Wittinghofer, A. (1993) *J. Biol. Chem. 268*, 923−929.
6. Feuerstein, J., Goody, R. S., and Wittinghofer, A. (1987) *J. Biol. Chem. 262*, 8455−8458.
7. Neal, S. E., Eccleston, J. F., Hall, A., and Webb, M. R. (1988) *J. Biol. Chem. 263*, 19718−19722.
8. Schweins, T., Scheffzek, K., Assheuer, R., and Wittinghofer, A. (1997) *J. Mol. Biol. 266*, 847−856.
9. Cherfils, J., and Chardin, P. (1999) *Trends Biochem. Sci. 24*, 306−311.
10. Hall, A. (1992) *Cell 69*, 389−391.
11. Hirshberg, M., Stockley, R. W., Dodson, G., and Webb, M. R. (1997) *Nat. Struct. Biol. 4*, 147−152.
12. Sillen, L. G., and Martell, A. E. (1971) *Stability constants of metal-ion complexes*, Suppl. 1, The Chemical Society, London.
13. De Weer, P., and Lowe, A. G. (1973) *J. Biol. Chem. 248*, 2829−2835.
14. Hall, A., and Self, A. J. (1986) *J. Biol. Chem. 261*, 10963−10965.
15. Hazlett, T. L., Moore, K. J. M., Lowe, P. N., Jameson, D. M., and Eccleston, J. F. (1993) *Biochemistry 32*, 13575−13583.
16. Webb, M. R., and Corrie, J. E. T. (2001) *Biophys. J. 81*, 1562−1569.
17. Eccleston, J. F., Kanagasabai, T. F., Molloy, D. P., Neal, S. E., and Webb, M. R. (1989) in *Guanine nucleotide binding proteins: common structural and functional approaches* (Bosch, L., Kraal, B., and Parmeggiani, A., Eds.) pp 87−97, Plenum, New York.
18. Corrie, J. E. T., Munasinghe, V. R. N., and Rettig, W. (2000) *J. Heterocycl. Chem. 37*, 1447−1455.
19. Newcombe, A. R., Stockley, R. W., Hunter, J. L., and Webb, M. R. (1999) *Biochemistry 38*, 6879−6886.
20. Brune, M., Hunter, J. L., Howell, S. A., Martin, S. R., Hazlett, T. L., Corrie, J. E. T., and Webb, M. R. (1998) *Biochemistry 37*, 10370−10380.
21. Leatherbarrow, R. J. (1992) *Grafit Version 3.0*, Erithacus Software Ltd., Staines, U.K.
22. Ivell, R., Sander, G., and Parmeggiani, A. (1981) *Biochemistry 20*, 6852−6859.
23. Latwesen, D. G., Poe, M., Leigh, J. S., and Reed, G. H. (1992) *Biochemistry 31*, 4946−4950.
24. Shimizu, T., Ihara, K., Maesaki, R., Kuroda, S., Kaibuchi, K., and Hakoshima, T. (2000) *J. Biol. Chem. 275*, 18311−18317.
25. Fletcher, A. N., and Bliss, D. E. (1978) *Appl. Phys. 16*, 289−295.
26. Hirshberg, M., Henrick, K., Haire, L. L., Vasisht, N., Brune, M., Corrie, J. E. T., and Webb, M. R. (1998) *Biochemistry 37*, 10381−10385.
27. Chaurasia, C. S., and Kauffman, J. M. (1990) *J. Heterocycl. Chem. 27*, 727−733.
28. Hutchinson, J. P., and Eccleston, J. F. (2000) *Biochemistry 39*, 11348−11359.
29. Boriack-Sjodin, P. A., Margarit, S. M., Bar-Sagi, D., and Kuriyan, J. (1998) *Nature 394*, 337−343.
30. Worthylake, D. K., Rossman, K. L., and Sondek, J. (2000) *Nature 408*, 682−688.
31. Eccleston, J. F., Hutchinson, J. P., and White, H. D. (2001) in *Protein ligand interactions: structure and spectroscopy. A Practical Approach Series* (Harding, S. E., and Chowdry, B. Z., Eds.) pp 201−237, Oxford University Press, Oxford, U.K.

BI0119464